

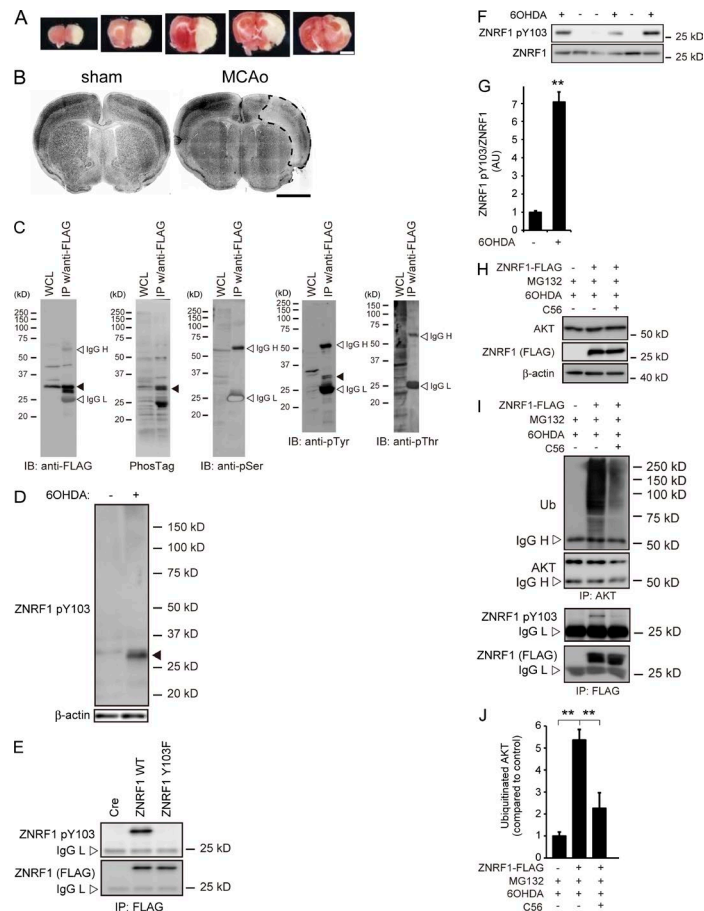
Wakatsuki et al., <http://www.jcb.org/cgi/content/full/jcb.201506102/DC1>

Figure S1. ZNRF1 is specifically phosphorylated at Y103 in neurons in response to 6OHDA in vitro and in vivo. (A and B) The MCAo model in this study. (A) Representative images of 2,3,5-triphenyltetrazolium chloride (TTC)-stained brain slices after MCAo in A. 6 d after MCAo, brains were sliced (1 mm) coronally, and stroke areas were visualized with 2% TTC staining at 37°C for 30 min. Tissues were then fixed in 4% PFA in PBS. In living tissue, TTC is enzymatically converted to 1,3,5-triphenylformazan, which is red in color, whereas it remains white in necrotic areas as a result of the lack of enzymatic activity. Bar, 1 mm. Note that the infarct area is identified by its white color. Reduced number of NeuN-positive neurons in the MCAo cortex. (B) 4 h after MCAo, brain tissues were fixed with 4% PFA and embedded in paraffin. 5- μ m-thick sections were collected and immunostained with an antibody against the neuron-specific nuclear protein NeuN in sham control (left) and MCAo (right) mouse brains. The area surrounded by dashed lines indicates the infarct core. Bar, 1 mm. (C) Phosphorylation of ZNRF1 on tyrosine residues in SHSY5Y neuroblastoma cells maintained with 6OHDA. SHSY5Y cells were transfected with WT ZNRF1 and maintained with 20- μ M 6OHDA for 3 h. After being cultivated for 24 h, cell lysates were analyzed by means of immunoprecipitation followed by immunoblots using specific antibodies against phosphoserine, phosphothreonine, and phosphotyrosine or Phos-Tag technology. Closed arrowheads indicate an immunoreactive band for the ZNRF1 protein. Note that ZNRF1 is significantly phosphorylated on tyrosine residues in cells maintained with 6OHDA. (D–G) Phosphorylation of ZNRF1 at Y103 in 6OHDA-lesioned neurons. (D) Cultured cortical neurons were treated with 20- μ M 6OHDA for 3 h. Cell lysates were subjected to an immunoblot analysis using antibodies against ZNRF1 pY103. Representative immunoblots are shown. The closed arrowhead indicates an immunoreactive band for ZNRF1 pY103. (E) The ZNRF1 Y103F mutant was resistant to phosphorylation in response to 6OHDA. Cultured cortical neurons were infected with the adenovirus vector expressing FLAG-tagged ZNRF1 WT or the ZNRF1 Y103F mutant and maintained with 20- μ M 6OHDA for 3 h. Cre-only expressing neurons served as a negative control for experiments. Cell lysates were subjected to immunoprecipitation with an anti-FLAG antibody and analyzed by immunoblotting. Note that ZNRF1 phosphorylation was significantly reduced by an amino acid substitution from tyrosine to phenylalanine at residue 103 of the ZNRF1 protein. (F and G) ZNRF1 pY103 immunoreactivity was detected in the brain lysate of the 6OHDA-lesioned animal model. Cell lysates were prepared from serial sections of the ipsilateral (+) or contralateral (–) striatum in the 6OHDA-lesioned animal model (3 h after the administration of 6OHDA) and subjected to an immunoblot analysis. Quantified levels of ZNRF1 pY103 normalized to the no-lesioned condition are shown in G ($n = 3$ in each group). The asterisks indicate a significant difference (two-tailed Student's t test; **, $P < 0.01$) from the no-lesioned condition. Note that ZNRF1 pY103 was only detected in damaged brain lysates. (H–J) EGFR inhibition blocks the phosphorylation of ZNRF1 at Y103 and the resultant increases in its activity ubiquitinate AKT in response to 6OHDA. (H and I) Cultured cortical neurons were infected with ZNRF1 WT, and treated with 6OHDA in the presence or absence of 20- μ M C56, an EGFR inhibitor, for 2 h followed by a treatment with MG132 for 16 h. Cre only expressing neurons served as a negative control (labeled as a dash for ZNRF1–FLAG). (H) Protein expression in 5% input of cell lysates was confirmed by an immunoblot analysis using antibodies against AKT or FLAG (for ZNRF1). β -Actin served as the loading control. (I) Cell lysates were subject to immunoprecipitation using antibodies against AKT, and the resultant immunoprecipitates were analyzed by immunoblotting (top). Expression levels of FLAG-tagged ZNRF1 WT and ZNRF1 Y103F in immunoprecipitates were also monitored using an anti-FLAG antibody and ZNRF1 pY103 (bottom). (J) Quantified levels for polyubiquitinated AKT normalized to β -actin are shown. $n = 5$. Significant differences from the control were determined by a one-way ANOVA with Tukey's post-hoc test. IB, immunoblot; IgG H, IgG heavy chain; IgG L, IgG light chain; IP, immunoprecipitate; Ub, ubiquitin; WCL, whole cell lysate.

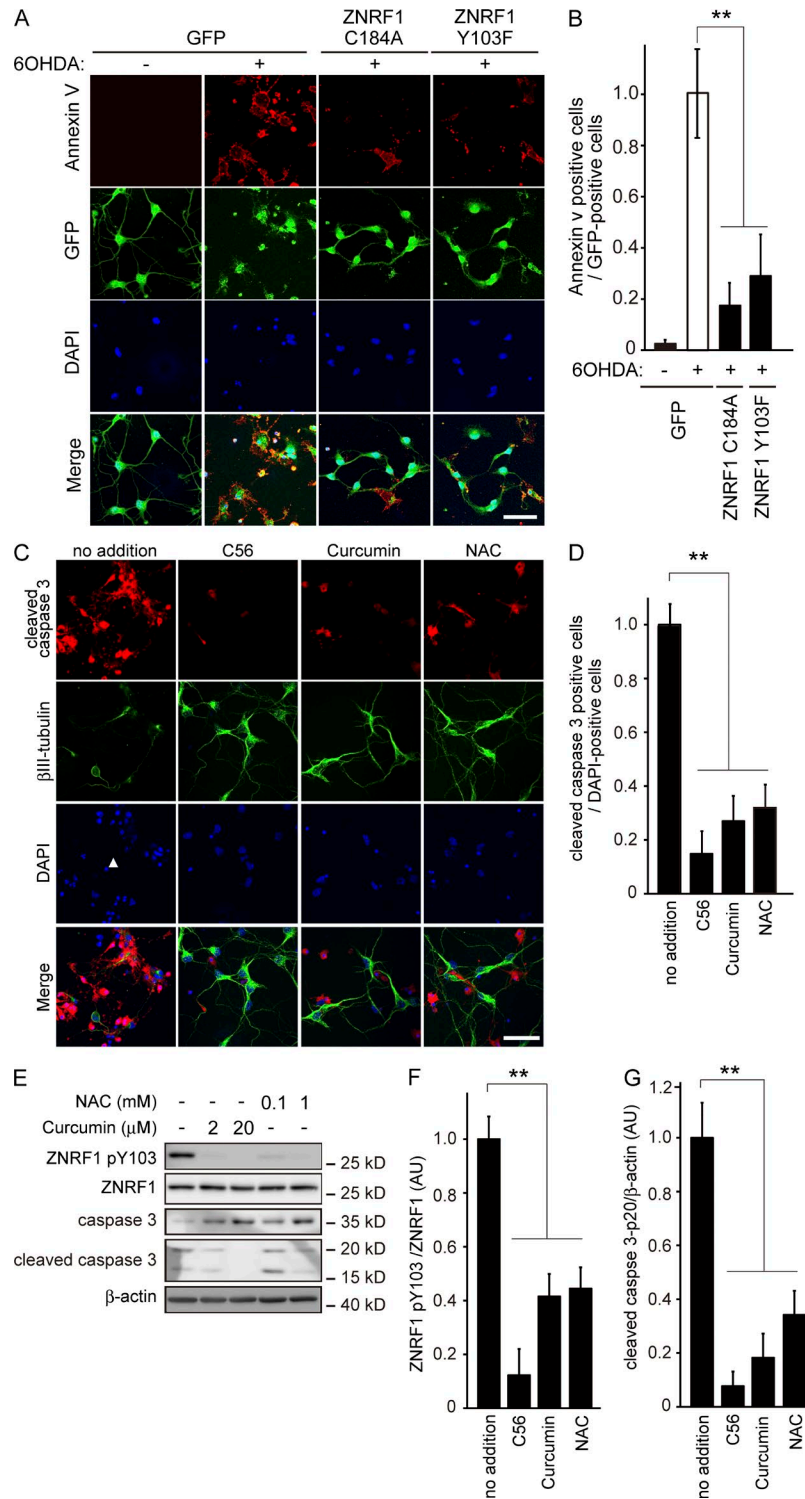


Figure S2. **Inhibition of ZNRF1 ubiquitin ligase activity protects primary cultured cortical neurons from oxidative stress-induced apoptosis.** (A and B) Primary cultured cortical neurons were infected with an adenovirus vector expressing GFP, FLAG-tagged ZNRF1 C184A, or ZNRF1 Y103F for 48 h and then treated with 20- μ M 6OHDA for 3 h. (A) Neurons were stained with 1 mg/ml Alexa Fluor 594-labeled annexin V for 15 min. annexin V binds to phosphatidylserine in the outer leaflet of the plasma membrane of cells, thereby starting the apoptotic process. Bar, 100 μ m. (B) The ratios of the annexin V-positive cell number to the total number of GFP-positive cells for each condition are shown relative to the ratio in the noninfected, 6OHDA-treated condition. (C–G) Representative photomicrographs for cleaved caspase 3 immunostaining are shown (C). Bar, 100 μ m. Nuclei and cell bodies were counterstained with DAPI and β III-tubulin, respectively. The arrowhead indicates one of the apoptotic nuclei. (D) The ratios of the cleaved caspase 3-positive cell number to the total number (the number of β III-tubulin-positive cells) for each condition relative to the no addition control are shown. (E–G) Immunoblot analyses for caspase 3, cleaved caspase 3, ZNRF1 pY103, and ZNRF1 were also performed. Shown are representative immunoblots (E), quantified expression levels for ZNRF1 pY103 normalized to ZNRF1 relative to the control level (F), and cleaved caspase 3 p20 normalized to β -actin relative to the control level (G). Data are presented as the mean \pm SEM. $n = 5$. Significant differences from the control (**, $P < 0.01$) were determined by a one-way ANOVA with Tukey's post-hoc test. AU, arbitrary units; NAC, *N*-acetyl-L-cysteine.

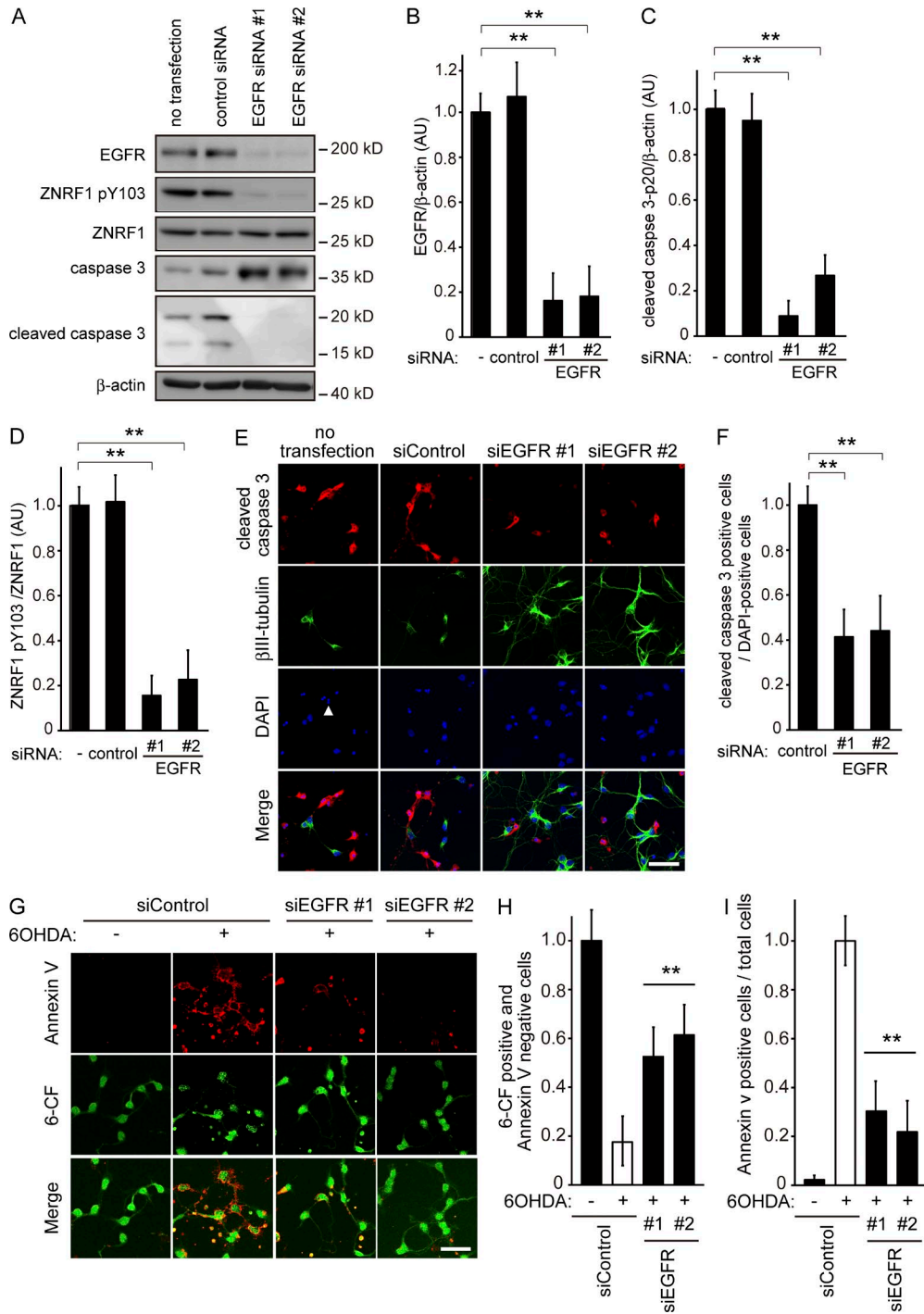


Figure S3. EGFR down-regulation protects primary cultured cortical neurons from 6OHDA-induced apoptosis. Cultured cortical neurons were transfected with siRNAs for EGFR, followed by a treatment with 6OHDA and were maintained for 24 h. Control siRNA-transfected neurons served as a negative control. (A–D) Immunoblot analyses for caspase 3, cleaved caspase 3, ZNRF1 pY103, and ZNRF1 were performed. Shown are representative immunoblots (A), quantified expression levels for EGFR normalized to β -actin relative to the level in the no transfection condition (B), cleaved caspase 3 p20 normalized to β -actin relative to the no transfection condition (C), and ZNRF1 pY103 normalized to ZNRF1 relative to the no transfection condition (D). $n = 5$. (E and F) EGFR down-regulation protects cultured cortical neurons from 6OHDA-induced apoptosis. Representative photomicrographs for cleaved caspase 3 immunostaining are shown (E). The nucleus and cell body were counterstained with DAPI and β III-tubulin, respectively. The arrowhead indicates one of the apoptotic nuclei. The ratios of the cleaved caspase 3-positive cell number to the total number of β III-tubulin-positive cells for each condition are shown relative to the ratio in the no transfection condition (F). $n = 5$. (G–I) Primary cultured cortical neurons were transfected with specific siRNAs for EGFR or the nontarget control and treated with 20- μ M 6OHDA for 3 h. (G) Neurons were stained with 1 mg/ml Alexa Fluor 594-labeled annexin V and 0.5-mM 6-CFDA for 15 min. The nonfluorescent compound 6-CFDA is hydrolyzed by esterases and converted to a fluorescent compound 6-carboxyfluorescein (6-CF) in living cells. Bar, 100 μ m. (H) The ratio of the 6-CF-positive and annexin V-negative cell number to the total cell number for each condition is shown relative to the ratio in the control condition (nontarget control siRNA transfected; 6OHDA treated). (I) The ratio of the annexin V-positive cell number to the total cell number for each condition is shown relative to the ratio in the control condition (nontarget control siRNA transfected; 6OHDA treated). Data are presented as the mean \pm SEM. Significant differences from the control (**, $P < 0.01$) were determined by a one-way ANOVA with Tukey's post-hoc test.

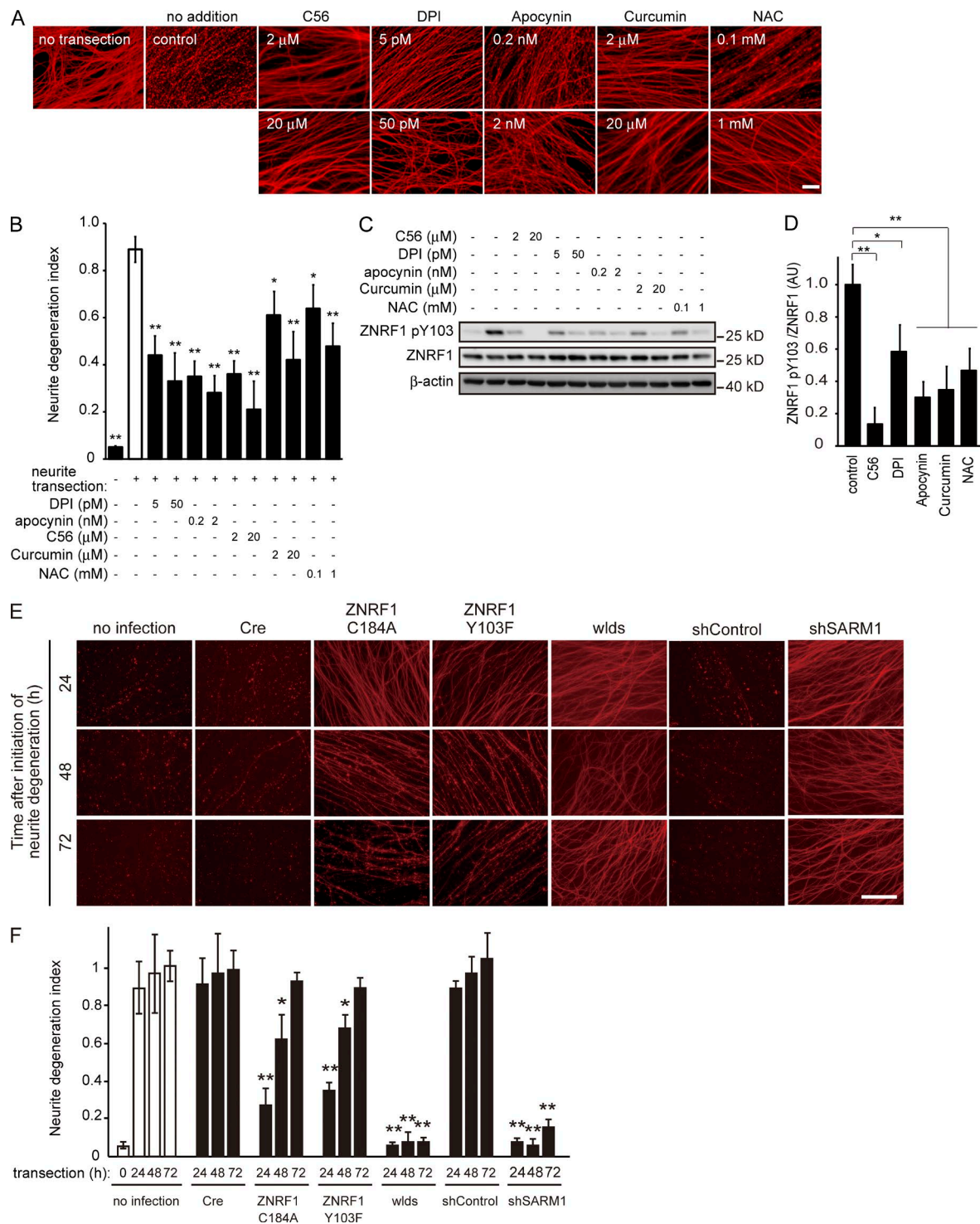


Figure S4. Progression of Wallerian degeneration is delayed by antioxidants, NADPH oxidase inhibitors, and an EGFR inhibitor. (A and B) The progression of Wallerian degeneration in cultured DRG neurons was inhibited by the antioxidants curcumin and NAC, the NADPH oxidase inhibitors DPI and apocynin, and the EGFR inhibitor C56. (A) Representative photomicrographs of β -tubulin immunostaining are shown. Bar, 25 μ m. (B) Neurite degeneration index values calculated for each condition at 24 h are shown. (C and D) An immunoblot analysis of ZNRF1 pY103 and ZNRF1 was performed against cell lysates prepared from neurites after neurite transection with or without the indicated reagents. Shown are representative immunoblots (C) and the quantified expression levels of ZNRF1 pY103 normalized to ZNRF1 and relative to the no addition condition (D). Data are presented as the mean \pm SEM. $n = 5$. Significant differences from the control (*, $P < 0.05$; **, $P < 0.01$) were determined by a one-way ANOVA with Tukey's post-hoc test. (E) The effects of the wlds mutation or expression of the indicated genes was assessed using an in vitro Wallerian degeneration model 24, 48, or 72 h after neurite transection. Representative photomicrographs for β III-tubulin immunostaining are shown. Bar, 50 μ m. (F) Neurite degeneration index values calculated for each condition at 24, 48, or 72 h are shown. The asterisks indicate a significant difference (a one-way ANOVA with Tukey's post-hoc test). *, $P < 0.05$; **, $P < 0.01$ from the no infection condition (open bars; labeled as control). Note that neurite integrity is maintained for up to 48 h by inhibiting ZNRF1 signaling, suggesting that the inhibition of ZNRF1 activity has a more modest effect on axonal protection than that of the expression of the Wlds protein or loss of SARM1, at least under this experimental condition. AU, arbitrary units; NAC, *N*-acetyl-L-cysteine.

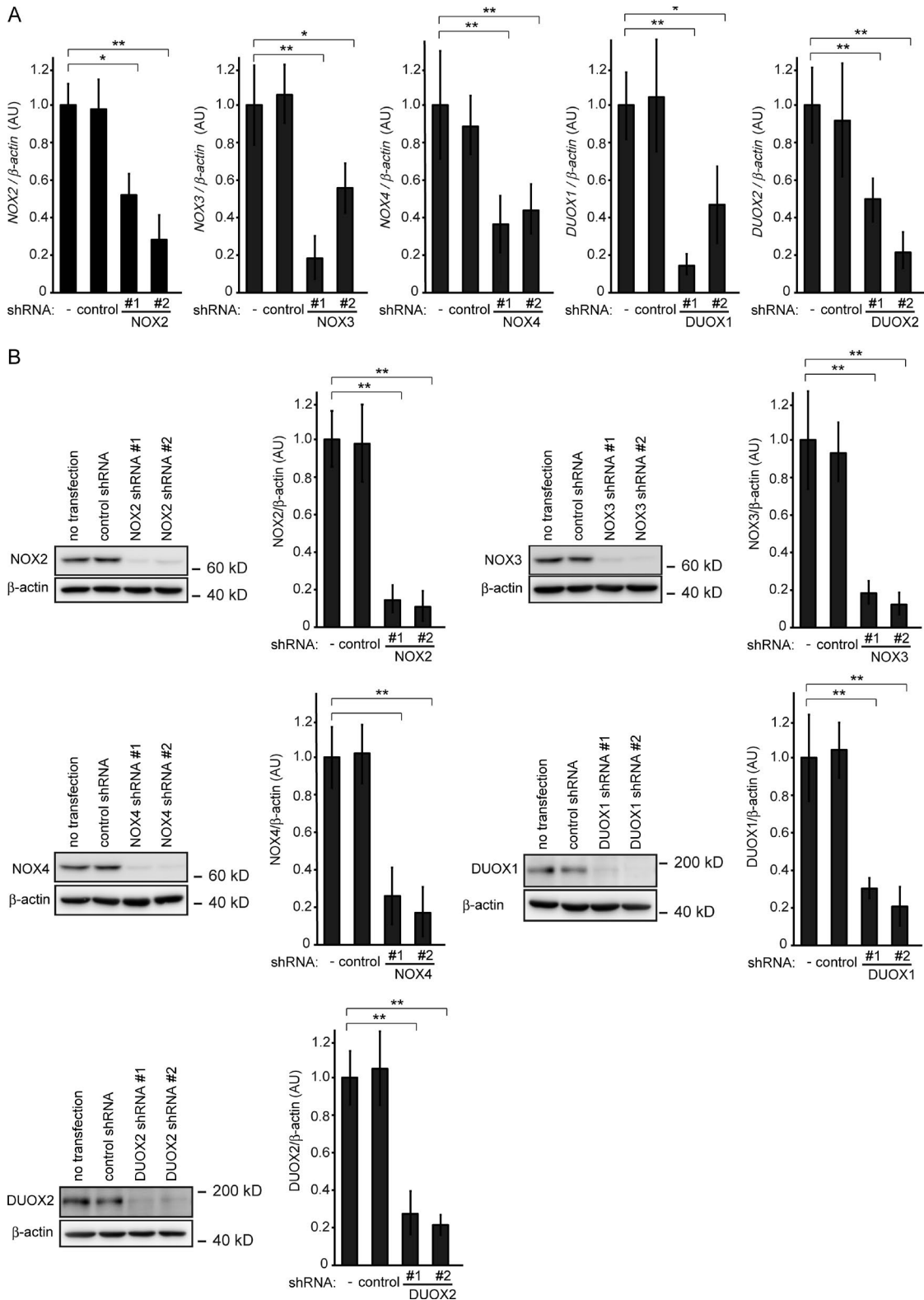


Figure S5. **Down-regulation of catalytic subunits of NADPH oxidases by specific shRNA in cultured DRG neurons.** The shRNA-mediated down-regulation of the indicated genes was performed in cultured DRG neurons via lentivirus vectors. The down-regulation of each molecule by the two independent shRNAs used in this study was confirmed by quantitative RT-PCR (A) or an immunoblot analysis (B). The expression levels of each molecule normalized to β -actin are shown relative to that of the no infection condition. Data are presented as the mean \pm SEM. $n = 5$. Significant differences from the control (*, $P < 0.05$; **, $P < 0.01$) were determined by a one-way ANOVA with Tukey's post-hoc test. AU, arbitrary units.